ISPRS Int. J. Geo-Inf. **2015**, *4*, 2379-2400; doi:10.3390/ijgi4042379

OPEN ACCESS

ISPRS International Journal of
Geo-Information
ISSN 2220-9964
www.mdpi.com/journal/ijgi

Article

Operational Monitoring of the Desert Locust Habitat with Earth Observation: An Assessment

François Waldner [1,*], Mohamed Abdallahi Babah Ebbe [2], Keith Cressman [3] and Pierre Defourny [1]

[1] Earth and Life Institue—Environment, Université catholique de Louvain, Croix du Sud 2, Louvain-la-Neuve 1348, Belgium; E-Mail: pierre.defourny@uclouvain.be

[2] Centre National de Lutte Antiacridienne, Nouakchott BP665, Mauritania; E-Mail: maouldbabah@yahoo.fr

[3] Desert Locust Information Service, FAO/AGP, Rome 00153, Italy; E-Mail: keith.cressman@fao.org

* Author to whom correspondence should be addressed; E-Mail: francois.waldner@uclouvain.be; Tel.:+32-10-473-680.

Academic Editor: Wolfgang Kainz

Received: 26 August 2015 / Accepted: 15 October 2015 / Published: 30 October 2015

Abstract: Desert locust swarms intermittently damage crops and pastures in sixty countries from Africa to western Asia, threatening the food security of 10% of the world's population. During the 20th century, desert locust control operations began organizing, and nowadays, they are coordinated by the Food and Agriculture Organization (FAO), which promotes a preventative strategy based on early warning and rapid response. This strategy implies a constant monitoring of the populations and of the ecological conditions favorable to their development. Satellite remote sensing can provide a near real-time monitoring of these conditions at the continental scale. Thus, the desert locust control community needs a reliable detection of green vegetation in arid and semi-arid areas as an indicator of potential desert locust habitat. To meet this need, a colorimetric transformation has been developed on both SPOT-VEGETATION and MODIS data to produce dynamic greenness maps. After their integration in the daily locust control activities, this research aimed at assessing those dynamic greenness maps from the producers' and the users' points of view. Eight confusion matrices and Pareto boundaries were derived from high resolution reference maps representative of the temporal and spatial diversity of Mauritanian habitats. The dynamic greenness maps were found to be accurate in summer breeding areas (F-score = 0.64–0.87), but accuracy dropped in winter breeding areas (F-score = 0.28–0.40). Accuracy is related

to landscape fragmentation (R^2 = 0.9): the current spatial resolution remains too coarse to resolve complex fragmented patterns and accounts for a substantial (60%) part of the error. The exploitation of PROBA-V 100-m images at the finest resolution (100-m) would enhance by 20% the vegetation detection in fragmented habitat. A survey revealed that end-users are satisfied with the product and find it fit for monitoring, thanks to an intuitive interpretation, leading to more efficiency.

Keywords: desert locust; habitat mapping; accuracy assessment; resolution bias

1. Introduction

The food security of sixty countries from Northern Africa to India is often threatened by desert locusts, *Schistocerca gregaria* (Forksål, 1775). This notorious insect pest [1] has the ability to form swarms of billions of individuals that damage crops and pastures. Their devastating effects lead to numerous socio-economic consequences for a tenth of the world population [2]. During the last invasion of 2003–2005, desert locust swarms have affected eight million people, mainly in Africa. Damages diminished harvest from 80%–100% [3]. To contain this pest, 13 million hectares have been sprayed in 26 countries. Costs, including food supply to affected populations, total a billion dollars [4].

Desert locusts exhibit a phase polyphenism in which behavioral, physiological and morphological traits change due to variations in the local population density [5,6]. Three mutually-interdependent and co-occurring phenomena lead to that transformation [7,8]: multiplication, population concentration and gregarization. Under these conditions, solitarious phase individuals shift to gregarious phase individuals that are more voracious and mobile. The gregarization density threshold varies according to development stages and is estimated at 250–500 adults locusts per hectare [9]. During remission, desert locusts are confined to arid and semi-arid areas of Africa, the Middle East and Southwest Asia, which covers 16 millions km^2. During outbreaks, on the other hand, desert locust swarms invade up to 29 million km^2 [10].

Desert locust control is part of FAO's original mandates [11]. FAO recommends a preventative strategy based on early warning and rapid response. This strategy implies continuously-updated information on the locust population status (field surveys), the ecological conditions (vegetation and soil moisture) and historical information (analogous situations in the past). Therefore, FAO operates the Desert Locust Information Service (DLIS) to ensure early warning of potential outbreaks by closely monitoring the meteorological and ecological conditions, as well as the locust populations. The breeding of desert locusts requires moist soil for egg laying and hatching, as well as green vegetation, providing food and shelter [12,13]. In arid areas, these conditions are associated with random and unpredictable rainfall events of more than 20 mm [14] and a greening of vegetation [15]. Earth observation systems can monitor those two factors at the continental level in a timely fashion. Complementary to field surveys, this technology proved itself even more valuable in remote areas, which are inaccessible or unsecured [16].

As the current spatial resolution of commercial satellites remains insufficient for direct detection of locusts [17], most research efforts have been devoted to map their potential habitat. In the 1970s, remote sensing brought new perspectives for mapping the preferential desert locust habitat, as well as monitoring the desert locust breeding areas [18]. Images from the Multispectral Scanner (MSS) onboard Landsat were analyzed visually and by means of digital image processing to monitor the locust habitat [19,20]. These images successfully detected the vegetation and monitoring of the photosynthetic dynamics. The Normalized Difference Vegetation Index (NDVI) has been intensively used to link vegetation and locust occurrence. Sinha and Chandra [21] adopted a visual approach to investigate the relationship of high NDVI areas with locust activity. Later, Hielkema *et al.* [22] demonstrated that an index based on the NDVI was correlated with rainfall and locust infestations in a region covering parts of Mali, Niger and Algeria between April and November 1980. Tappan *et al.* [23] presented a method for identifying favorable conditions for desert locust and Senegalese grasshopper egg incubation based on local area coverage imagery from NOAA-AVHRR. They concluded that occurrences of high NDVI values correspond to the emergence of vegetation, which can be further exploited to monitor the reproduction areas of locusts. Despland *et al.* [24] used NOAA-AVHRR satellite imagery to relate the abundance and spatial distribution of resources at the landscape scale to historical records of outbreaks. They showed also the difference in the spectral response of vegetation growing near the Red Sea compared to Mauritania. Cherlet *et al.* [25] suggested an NDVI threshold of 0.14 to discriminate vegetation from bare soil. This threshold is applied on a mosaic of SPOT-VGT images covering the entire desert locust distribution area. This technique yielded an acceptable result with the detection of the most homogeneous events. However, in certain areas, favorable areas are omitted with such a threshold, particularly those with sparse vegetation with a low leaf area index. In order to reduce those omissions, 250-m TERRA-MODIS images have been coupled to 1-km SPOT-VEGETATION images [26]. This combination allows reducing the omission errors thanks to MODIS's higher spatial resolution. Furthermore, commission errors were reduced thanks to the MODIS moderate infrared (MIR) band. Vegetation detection for desert locust habitat mapping with the NDVI seems to exhibit limitations [26–29]. This is even more constraining in recession areas, where NDVI sensibility to the soil background becomes critical [27]. Indeed, certain bare soils have spectral characteristics in the red (R) and the infrared (IR) that induce NDVI values inseparable from sparse vegetation [24,26]. Operationally, they translate into false alarms, that is vegetation detection where there is none, that must be eliminated to provide accurate information to the National Desert Locust Control Units [26].

In collaboration with FAO, Pekel *et al.* [30] addressed the need for a reliable vegetation indicator in arid areas. They proposed a fully-automated multitemporal approach based on a colorimetric transformation to discriminate vegetated areas in near real time. To ensure a robust discrimination of green vegetation, three spectral bands are combined: red (R), near infrared (NIR) and MIR. The latter, particularly sensitive to water content in soil and vegetation, brings complementary information to the two other bands [31]. Given the limitations of the NDVI in arid and semi-arid areas and those of the RGB color space, a colorimetric transformation was applied to project the reflectances into the HSV color space (hue, saturation and value). In this color space, hue appears as a qualitative spectral index, and its temporal variations can be interpreted as a land cover change [32]. The detection method is based on a set of thresholds that jointly use the hue and the

NDVI to distinguish vegetation from non-vegetation (*i.e.*, all other land cover types). The thresholds were identified through an empirical and statistical approach that relies on an exhaustive sampling (by photo-interpretation) of pixels distributed spatially and temporally. In case of ambiguous membership to one class or the other, the temporal pixel trajectory defined by Hue_{slope}, the difference between the current and the previous hue values, evaluates the belonging of a pixel to the vegetation class. Indeed, soil pixels are expected to oscillate continuously around their actual value according the signal-to-noise ratio, whereas vegetation pixels progressively migrate to the unambiguous area as vegetation is growing. The colorimetric transformation and the decision rules are applied on 10-day mean composited images [33]. The final product integrates a temporal components thanks to a time meter that accounts for the number of decades a pixel has been tagged as vegetation (Figure 1). A color table allows an intuitive and straightforward identification of ephemeral (red), seasonal (light green) and perennial vegetation (dark green). This provides operationally and in almost real time a user-friendly vegetation dynamic map updated every 10 days over the whole desert locust area. Those areas in which vegetation has become green in the past one to two decades are the most important for desert locust, as they prefer annual vegetation that is becoming green. Areas that are consistently green over time probably consist of perennial vegetation (oases, forests, *etc.*) that are less suitable for desert locusts. Large contiguous areas are more important than isolated pixels. The operational implementation of this method provides products to improve the desert locust monitoring and early warning in Africa and Asia, known as dynamic greenness maps. Since July 2010, these maps are freely available to the National Locust Control Centers (NLCCs) and the FAO on the DevCoCastportal. More recently, Renier *et al.* [34] developed a dynamic vegetation senescence indicator for near-real-time monitoring of the desert locust habitat with MODIS in order to identify areas likely to be abandoned by locusts.

This article aims at assessing the accuracy in space and time of the dynamic greenness map product developed by Pekel *et al.* [30]. To this end, it examines several aspects of the product efficiency to map the potential habitat of the locust. First, a traditional accuracy assessment quantifies the producers' and users' accuracy by means of a wall-to-wall comparisons of the product with reference maps derived from 30-m Landsat data. Second, the effect of spatial resolution and habitat fragmentation on the accuracy is studied. In particular, three resolutions are investigated: 1-km (SPOT-VEGETATION), 250-m (MODIS) and 100-m (PROBA-V). They correspond to the resolution of past, current and potential sensors for the application. Finally, an end-user survey assesses the fitness for the purpose and integration of the dynamic greenness maps in the monitoring and control activities.

2. Material

2.1. Study Area

The study focuses on Mauritania, which covers 1,030,700 km^2 in northwest Africa (Figure 2) between 15–27 degrees N and 15–17 degrees W. The Sahara covers the north and Sahel borders the south of the country. Herbaceous and shrub vegetation grows in the semi-arid region, whereas sparse vegetation dominates the arid region. Climate is characterized by a short rainy season occurring during July–September, as well as a north-south gradient of the mean annual rainfall [35].

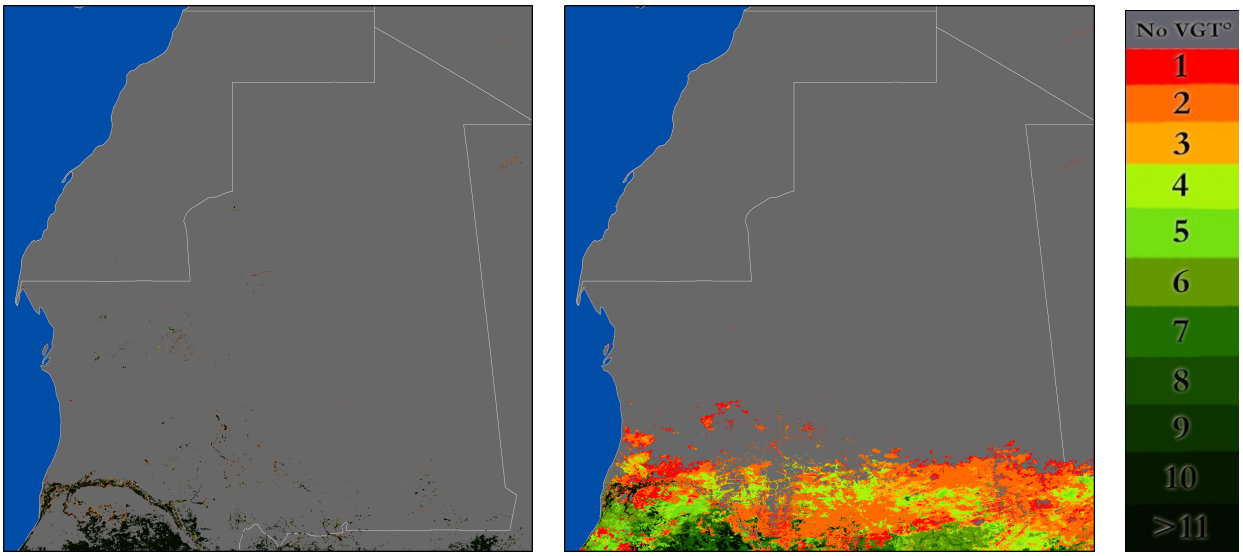

(**a**) (**b**) (**c**)

Figure 1. Dynamic greenness map products for Mauritania on two contrasted dates: (**a**) second decade of February 2011; and (**b**) first decade of September 2011; (**c**) the color code of the time meter. This illustrates the spatial-temporal variability of vegetation and the vegetation response to seasonal rainfall. The product with its time meter flags priority areas to be surveyed (warm colors) because of a recent greening of vegetation becoming suitable for locusts, as they prefer fresh vegetation. On the contrary, dark-colored areas present a lower interest for locusts.

Historically, livestock farming is the dominating activity (80% of agricultural activities and 22% of the gross national product) [36], followed by crop farming and exploiting forest resources for logging and energy [37,38]. Agriculture mostly takes place in the south of the country, and irrigated crops are limited to the surroundings of the Senegal River [39]. In the north, pastoral activities are dominated by camel and sheep holdings; crops are only found in oases.

2.2. Satellite Data and Reference Datasets

Accuracy assessment relies on an independent dataset of ground truth to be compared to the map to validate. High resolution images are commonly taken as proxies for ground truth data, as a robust sampling is often difficult to obtain with actual *in situ* data [40]. In this study, both sources of data were combined.

First, a ground truth dataset was collected as a result of field survey in southwestern Mauritania during August and September 2012. A plethora of methods have been developed to estimate vegetation density [41,42]. Because of the large areas to cover, vegetation density was here estimated by point-intercept transects [43]. Density was determined by the percent of rigidly-located vertically-projected points that encounter vegetation: trees, bushes, shrubs and grasses. Points were spread regularly at meter intervals along a 100-m transect.

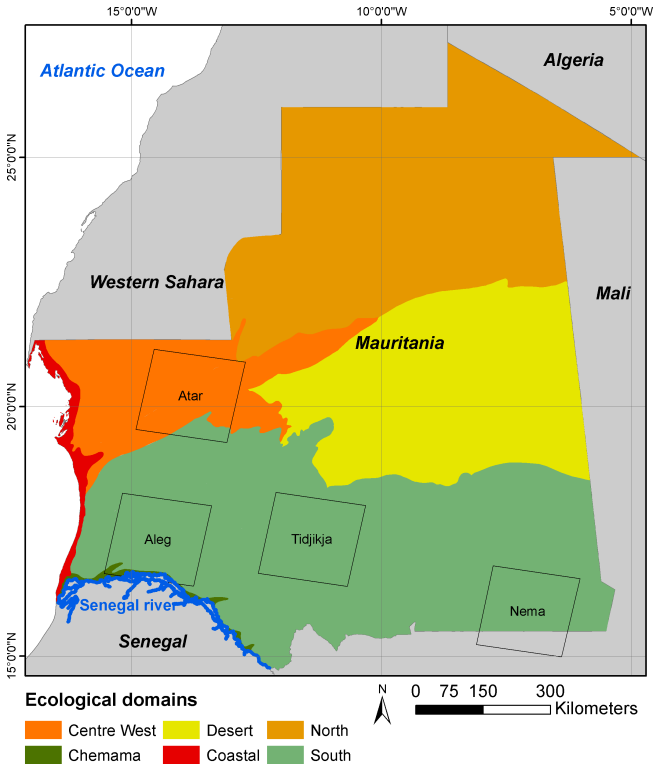

Figure 2. Mauritania and its six ecological domains. Two observations on the four study sites ensure a robust spatial-temporal sampling. Summer breeding areas cover the south domain below the 18th parallel. In the spring and the winter, locusts breed in favorable areas of the north and the center-west domains.

Second, high resolution Landsat imagery was downloaded in four regions of interest that were selected in light of the Mauritanian territory apportionment in ecologically homogeneous units [44] (Figure 2). Within the available Landsat archive, eight cloud-free Landsat-5 TM images were selected: two per site at dates falling into the rainy and the dry season in relevant regions for desert locust monitoring (Table 1). Training samples of vegetation and non-vegetation were generated based on photo-interpretation, expert-knowledge of the areas, existing land cover maps and punctual survey information of the RAMSES database (Recognition And Monitoring System of the Environment of Schistocerca) database. RAMSES compiles field observations collected by locust survey teams since 1988 and provides information on vegetation (species, density, phenological stages, *etc.*), locust (density, stages, *etc.*) and other relevant physical parameters for locust development, such as soil humidity. Then, the widely-used supervised maximum likelihood classification was applied to the red, the near infrared and the moderate infrared TM bands to produce reference binary vegetation maps (Figure 3). As the algorithm ran on a pixel basis, it neglected the textural and contextual information, and a characteristic salt and pepper effect affected the maps. To tackle this issue, four 3×3 morphological opening filters (one vertical, one horizontal and one in each diagonal direction) were applied on the classified maps.

Finally, the dynamic greenness maps corresponding to the reference data were downloaded from the DevCoCast portal in addition to those covering the field campaign period.

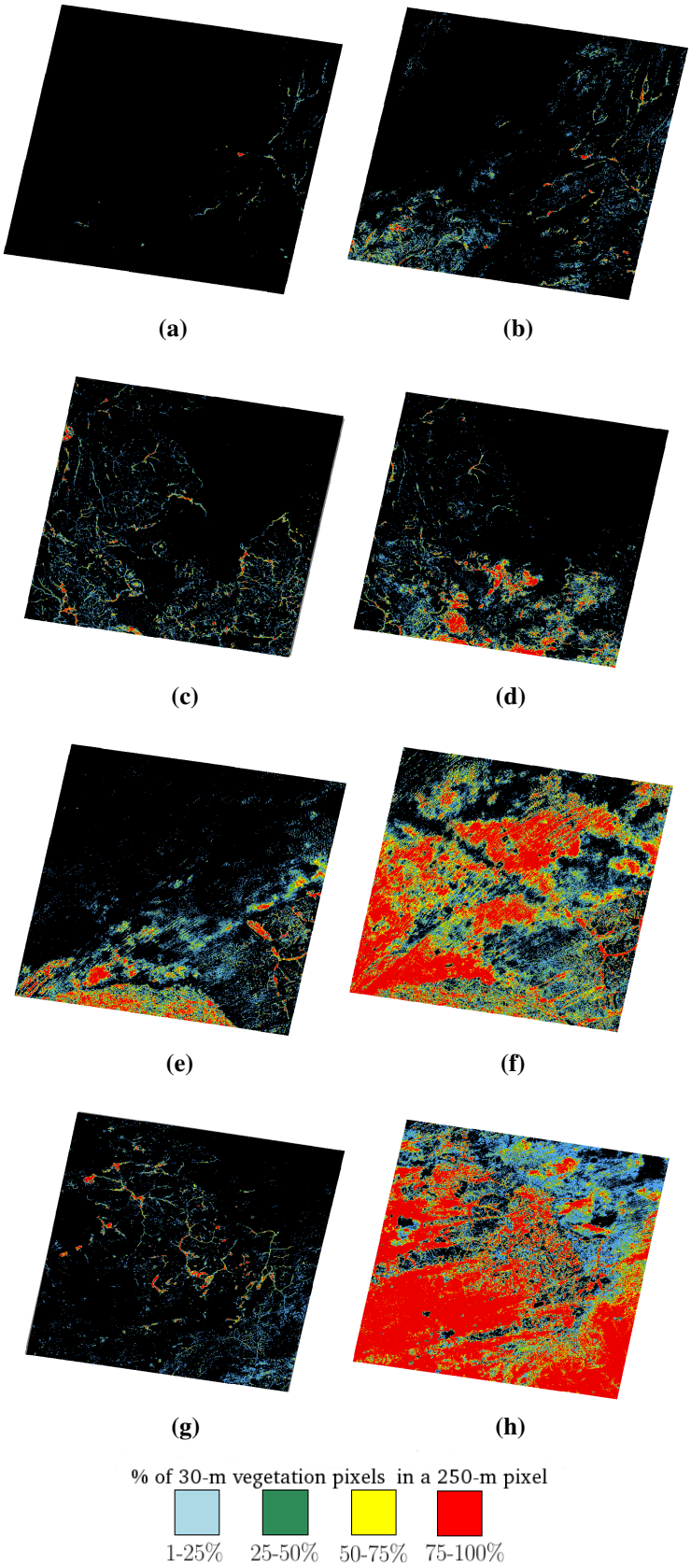

Figure 3. Percentage of vegetation in the reference maps aggregated at 250 m: (**a**) center-west 20 February 2010; (**b**) center-west 19 November 2010; (**c**) south Tidjikja 21 January 2010; (**d**) south Tidjikja 29 July 2009; (**e**) Chemama 20 February 2010; (**f**) Chemama 19 November 2010; (**g**) south Nema 17 February 2010; (**h**) south Nema 12 October 2009.

Table 1. Characteristics of the images for the eight study sites including the acquisition dates of the Landsat images and of the Dynamic Greenness Maps (DGM) along with the vegetated area (Veg. Area). There is a large dominance of the non-vegetation class in the dry season and in the northern areas.

Zone	Row-Path	Date Landsat	Dekade DGM	Veg. Area (ha)	Veg. Area (%)
Atar	204-046	2010/02/20	2010/02/11	4027	0.12
		2010/11/19	2010/11/11	57,777	1.71
Tikjikja	202-048	2010/01/21	2010/01/21	150,388	4.43
		2009/07/29	2009/08/01	176,496	5.29
Aleg	204-048	2010/02/20	2010/02/11	234,880	7.01
		2010/11/19	2010/11/11	1,273,143	37.30
Nema	199-049	2010/02/17	2010/02/21	63,278	1.91
		2009/10/12	2009/10/11	1,780,856	53.99

3. Methods

The methodology relies on two main components: (1) a quantitative assessment of the accuracy of the maps; and (2) the assessment of its fitness and usability by the users. In the first component (Figure 4), greenness maps are validated wall-to-wall using the high resolution reference vegetation maps degraded at 250 m. Because of the resampling, high resolution reference vegetation maps degraded at 250 m provided continuous vegetation density information. *In situ* data were thus combined to greenness maps to identify the optimal vegetation density threshold to apply on the degraded reference maps. The high resolution maps served in the second step to assess the low resolution and to relate the accuracy to the landscape fragmentation.

3.1. Traditional Accuracy Assessment

The greenness maps were first validated by means of confusion matrices [45]. A confusion matrix is a square matrix that compares a classified map to reference data. Diagonal values represent the agreement between the reference and the classification, while non-diagonal values represent the errors. Traditional accuracy measures were derived from the error matrix, namely the omission errors (OE) and commission errors (CE), the overall accuracy (OA), the Kappa statistic (κ) and the F_1-score [46–49].

The overall accuracy (OA) expresses the probability of a randomly-selected pixel to be classified accurately. The Kappa statistic, an alternative to the OA, takes into account the random agreement [47,50]. It measures the proportion of agreement after correction of random chance agreement [51].

$$\mathrm{OA} = \frac{\sum_{i=1}^{k} n_{ii}}{n} \tag{1}$$

$$\kappa = \frac{\sum_{i=1}^{k} n_{ii} - \sum_{i=1}^{k} n_{i+} n_{+i}}{n^2 - \sum_{i=1}^{k} n_{i+} n_{+i}} \tag{2}$$

where n is the amount of observation, n_{ii} the diagonal agreements between row i and column i and n_{i+} and n_{+i} are the marginal totals of row i and column i, respectively. For a specific class, the omission

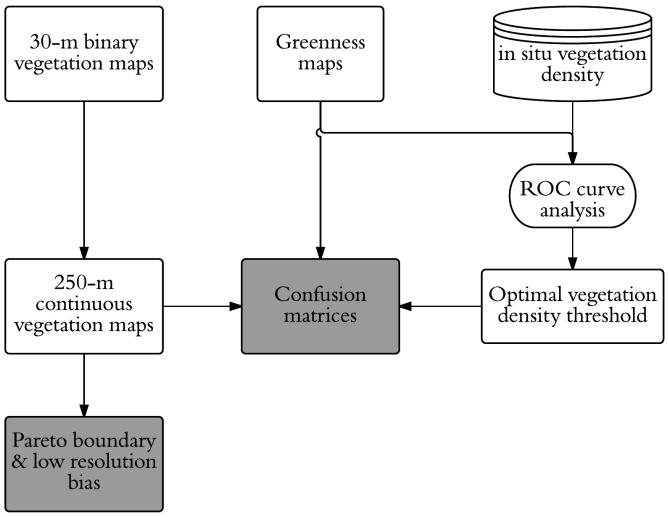

Figure 4. Flowchart of the accuracy assessment. The analysis of the ROC curve built with the greenness maps and *in situ* observation allowed defining an optimal vegetation threshold for detection. This threshold was then applied to continuous vegetation reference maps degraded at 250 m to derive confusion matrices for the greenness maps. The Pareto boundary was also computed thanks to the continuous vegetation reference maps, which permitted identifying the part of the error solely due to the resolution.

error is the rate of pixels incorrectly left over, whereas the commission error is the rate of incorrectly included pixels. These two error types are linked to the producer and user accuracy (1-PA and 1-UA), respectively. The F-score [48] is a synthesis accuracy indicator to be interpreted as the harmonic mean of the producer accuracy and the user accuracy [52]. This study used the F_1-score computed as:

$$F_1\text{-score} = \frac{2 \times UA \times PA}{UA + PA} \quad (3)$$

The confusion matrices were derived from the wall-to-wall comparison of the dynamic greenness maps with their respective high resolution reference maps degraded to the MODIS resolution grid. However, because of the resampling, the reference maps have a continuous field scale legend (percentage of 30-m vegetation pixels in a 250-m pixel). A threshold had to be applied to generate a binary low resolution reference map. Instead of using a majority rule, the identification of the optimal cut-off relied on the receiver operating characteristic (ROC) curve. The ROC curve analysis for two classes plots the true positive rate (TPR) on the y-axis and their equivalent false-positive rate (FPR) on the x-axis for every possible cut-point [53]. The area under the curve (AUC) provides a single measure of the probability that the classifier will rank a randomly-chosen positive instance higher than a randomly-chosen negative instance [54]. The value of the AUC ranges between 0.5 and 1, 0.5 corresponds to the level of accuracy reached by random chance. To construct the ROC curve, each transect vegetation density was related to its class as detected by the greenness maps, and accuracy was evaluated at regularly-spaced cut-off values. To identify the optimal cut-off value, this study utilizes the Youden index that maximizes the distance to the identity (diagonal) line [55].

3.2. Effect of the Spatial Resolution on the Accuracy

3.2.1. The Pareto Boundary

Confusion matrices do not consider the contextual influence of mixed pixels on the product accuracy [40]. Besides, when validating a coarse resolution product with a high resolution reference map, the assumption of equal spatial resolution between the reference and the product is violated. The Pareto boundary method is an alternative to deal with these shortcomings. The number of low resolution pixels covering multiple classes is closely linked to the ground features (reference data) and is a function of their shape, size and spatial patterns [56,57]. The difference in spatial resolution between high and low resolution data is referred to as the low -resolution bias [40]. The resolution bias sets down the omission and commission errors as conflicting objectives. Effectively, residual error after classification cannot be avoided. Any attempt to reduce the commission errors will inevitably lead to an increase of the omission errors and conversely. Therefore, in the OE/CE bi-dimensional space, a region of unreachable accuracy limited by the Pareto boundary separates the errors due to the spatial resolution and the method. The Pareto boundary determines the maximum user and producer accuracy values that could he attained jointly and represents such a lower limit as a boundary. It usefulness has already been demonstrated for assessing various classifications, e.g., burnt areas [58], snow products [59] and cropland identification [60]. To generate the Pareto boundary, the high resolution reference map is degraded to the low resolution pixel size. Each new pixel value corresponds to the percentage of high resolution pixels of the class of interest. A set of low resolution products is obtained by thresholding the low resolution reference map. For each threshold defining the percentage for which a pixel is considered as vegetation, the pair of efficient error rates OE/CE is computed. The line joining all of these points defines the Pareto boundary of a specific high resolution reference to a defined low resolution pixel size. The distance between the product and the boundary indicates the performance of the method. The area under the efficient solution curve indicates the accuracy of the detection algorithm.

The Pareto boundary was generated for the eight Landsat reference images at three resolutions: 1-km, 250-m and 100-m, which corresponds to the spatial resolution of SPOT-VEGETATION, MODIS and PROBA-V (at nadir), respectively. These resolutions represent the backup, the current and the potential future sensors used for the product. To account for misregistration in superimposing the low and high resolution grids [40], 100 random shifts were generated within the range of +/−0.5 pixels of low resolution data. The corresponding variance of the omission and commission errors were computed for one of the test sites.

Finally, the potential improvements of the integration of 100-m PROBA-V images into the processing chain was investigated. Pareto boundaries for 100-m spatial resolution were derived for the eight reference images. The potential reduction of the unreachable region (PRUR) was calculated for each image i:

$$\text{PRUR}_i = 100 \times \left(1 - \frac{\text{Unreachable Region Area at 100-m for image } i}{\text{Unreachable Region Area at 250-m for image } i}\right) \quad (4)$$

3.2.2. Habitat Structure

Habitat structure is one of the primary factors involved in promoting crowding among solitarious phase locusts [61]. Since the efficient solution of the boundary is affected by the pixel size, the landscape distribution of vegetation should also affect the accuracy. Hence, the coarser the resolution of pixels with a low percentage of vegetation, the stronger the effect of the resolution bias and the less accurate the vegetation detection [40]. Landscape patterns are described by the statistical distribution of the size and the shape of patches and their spatial arrangement. A large number of metrics and indices have been developed to characterize the landscape composition and the configuration [62]. In this study, the landscape fragmentation was studied by means of the edge density ratio (ED). ED measures the linear distance of the border by the unit of the surface. A large ratio indicates that pixels of the class of interest (here, vegetation) are generally close to edges. Monod [63] defined two modes for vegetation in the Saharan environment: diffuse (continuous) and contracted (discontinuous). In more arid environments, vegetation is contracted and confines itself in wadis or depressions, where topography concentrates the water. In general, contracted vegetation is characterized by a higher ED than diffuse vegetation.

3.3. End-User Survey

National locust information officers of twenty countries replied to a questionnaire prepared by FAO DLIS. This survey sought to evaluate the fitness and the integration of dynamic greenness map in the decision making process for interpretation of the ecological situation and planning the field operations and reporting. It also compared the greenness maps to other satellite data used for analysis (e.g., rainfall estimates).

4. Results

4.1. Accuracy Assessment

To deal with the difference in spatial resolution between the reference data and the product, the spatial resolution of the reference is often aggregated to match the product's. To set an appropriate class percentage threshold, the ROC curve analysis was applied (Figure 5). The Youden index determined 47% of vegetation density as the optimal cut-off value. Besides, the area under the curve reaches 84.9%, which corresponds to a good accuracy compared to a random classifier (50%).

Taking the optimal cut-off value, confusion matrices were calculated for the eight cases (Table 2). In general, the overall accuracy is around 95% due to the large agreement between non-vegetation pixels. Kappa statistics suggest low change agreement. Large omission and commission errors are observed for the vegetation class during the dry season and also during the rainy season for the arid regions (Atar and Tikjikja). These errors are drastically reduced when considering well-watered regions during the rainy season (Nema and Aleg). In fact, they display a north-south gradient of accuracy mimicking that of rainfall.

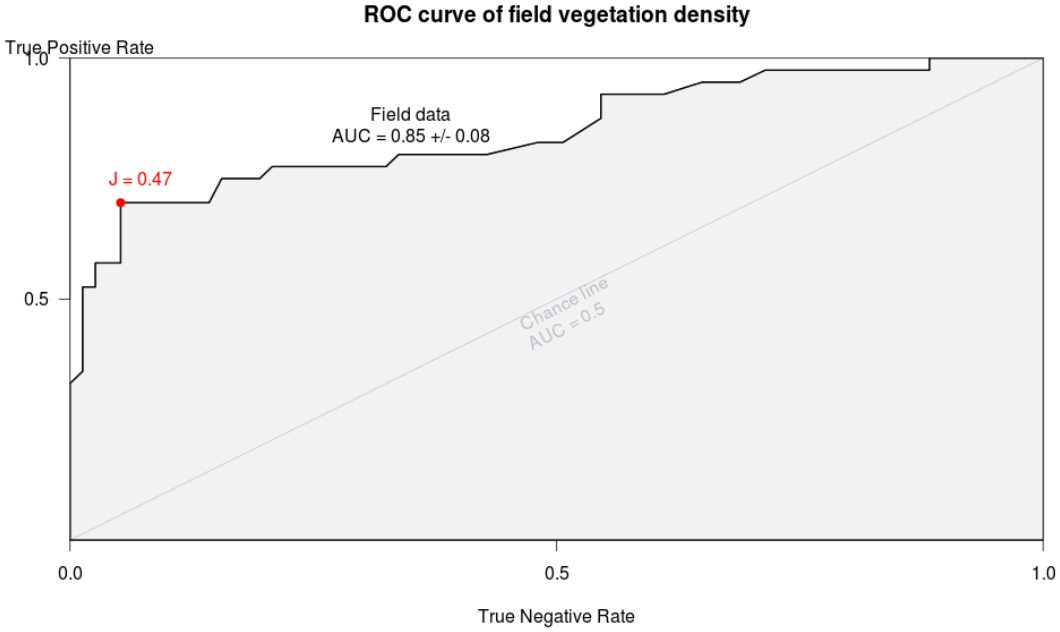

Figure 5. ROC curve for the field vegetation density (n = 113). The best cut-off value (in red) corresponds to the optimal percentage of vegetation coverage for detection. The Youden index J identifies the threshold to be further used in the computation of the error matrices. The AUC of 84.9% indicates good performance compared to a random classifier.

Table 2. Accuracy measures for the eight confusion matrices and the corresponding edge density metric. High overall accuracy is observed, but is strongly influenced by the agreement of non-vegetation pixels. During the dry season, omission and commission errors approach 60%–70% for every scene, but during rain, errors are reduced according to the north-south rainfall gradient. ED, edge density; OE, omission error; CE, commission error.

Zone	Season	ED (m/ha)	OE (%)	CE (%)	F-Score	OA (%)	Kappa
Atar	Dry	273	67.8	75.3	0.280	99.8	0.278
	Rainy	308	72.3	71.8	0.279	97.4	0.267
Tikjikja	Dry	247	62.7	73.8	0.307	96.4	0.290
	Rainy	200	61.9	54.4	0.415	93.9	0.384
Aleg	Dry	224	63.7	49.3	0.423	92.6	0.384
	Rainy	167	41.5	29.0	0.641	74.2	0.443
Nema	Dry	261	68.1	73.1	0.291	96.9	0.276
	Rainy	86	9.7	16.5	0.867	82.7	0.620

The dynamic greenness maps were further analyzed with the Pareto boundary method (Figure 6) at 1 km, 250 m and 100 m, corresponding to the spatial resolution of SPOT-VEGETATION, MODIS and PROBA-V. At 250 m, the unreachable region appears to have a substantial impact, accounting for up to 60% of the errors during the dry season. Its influence diminishes along with latitude during the rainy season. The variance of the Pareto boundary resulting from the uncertainties when superimposing the two grids is always below 0.01 and thus negligible.

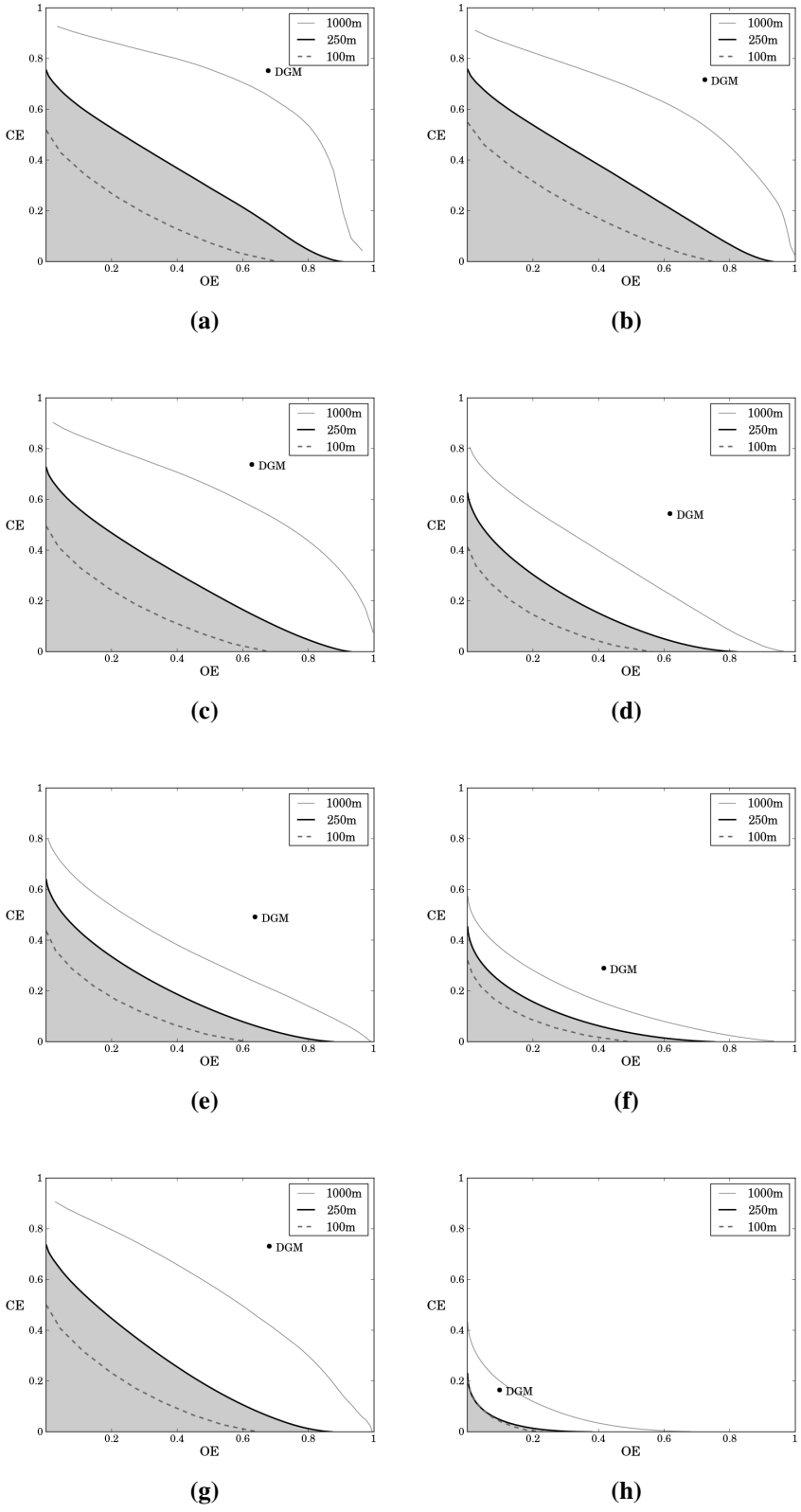

Figure 6. Pareto boundaries for the eight reference maps and the simulated boundaries for the SPOT-VEGETATION (1000 m), MODIS (250 m) and PROBA-V(100 m) sensors. In the current 250-m product, the unreachable region accounts for up to 60% of the errors. (**a**) Atar, dry season; (**b**) Atar, rainy season; (**c**) Tidjikja, dry season; (**d**) Tidjikja, rainy season; (**e**) Aleg, dry season; (**f**) Aleg, rainy season; (**g**) Nema, dry season; (**h**) Nema, rainy season.

The edge density metric was calculated for each reference map (Table 1). ED, reflecting both the complexity and the shape of the habitat, is linearly correlated to the accuracy (R^2 = 0.9) (Figure 7). Low classification accuracy (F_1-score < 0.5) occurs for regions with fragmented landscapes (>200 m/ha). In contrast, large vegetation patches (<150 m/ha) are mapped with a higher accuracy.

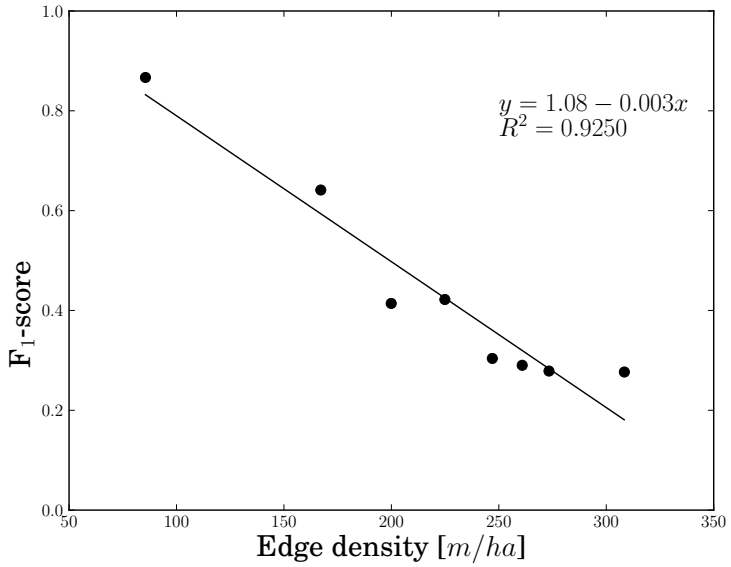

(a)

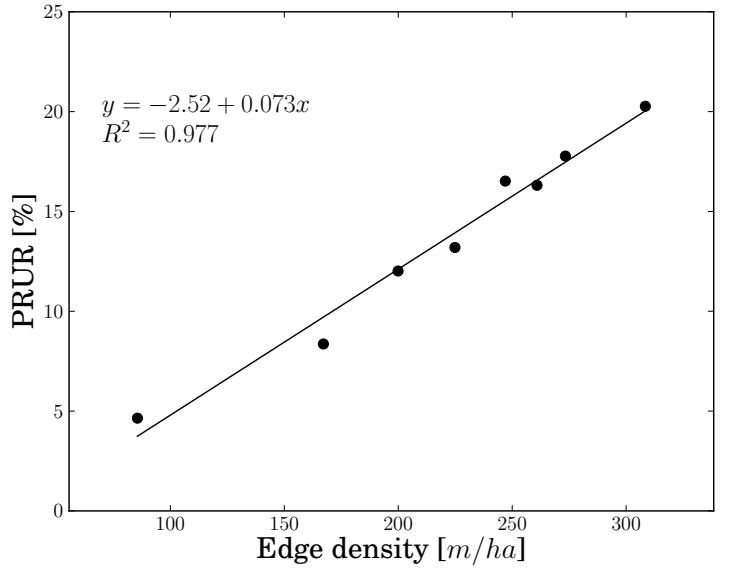

(b)

Figure 7. (**a**) Habitat fragmentation is an indicator of the achieved accuracy. The higher the fragmentation, the lower the accuracy rate. (**b**) Simulated reduction of the unreachable region for a spatial resolution of 100 m corresponding to that of PROBA-V. In a fragmented habitat, a product at 100 m would reduce the low -resolution bias by 20%.

The improvements of the integration of the 100-m PROBA-V images in the processing chain was estimated by the potential reduction of the unreachable region. The results provide support for the view

that the spatial resolution critically constrains the mapping accuracy (Figure 7). The PRUR is linearly related to the ED (R^2 = 0.97): the more fragmented the habitat, the larger the potential reduction. In fragmented habitat, such as in Atar, a product at 100 m would reduce the low resolution bias by 20%.

4.2. End-User Assessment

National information officers have filled in an on-line questionnaire. Survey results show that dynamic greenness maps are successfully addressing the users (Figure 8). They indicated that the dynamic greenness maps are easy to download and to analyze compared to reflectance images and rainfall estimate products. However, users expressed concern about the timeliness of the product.

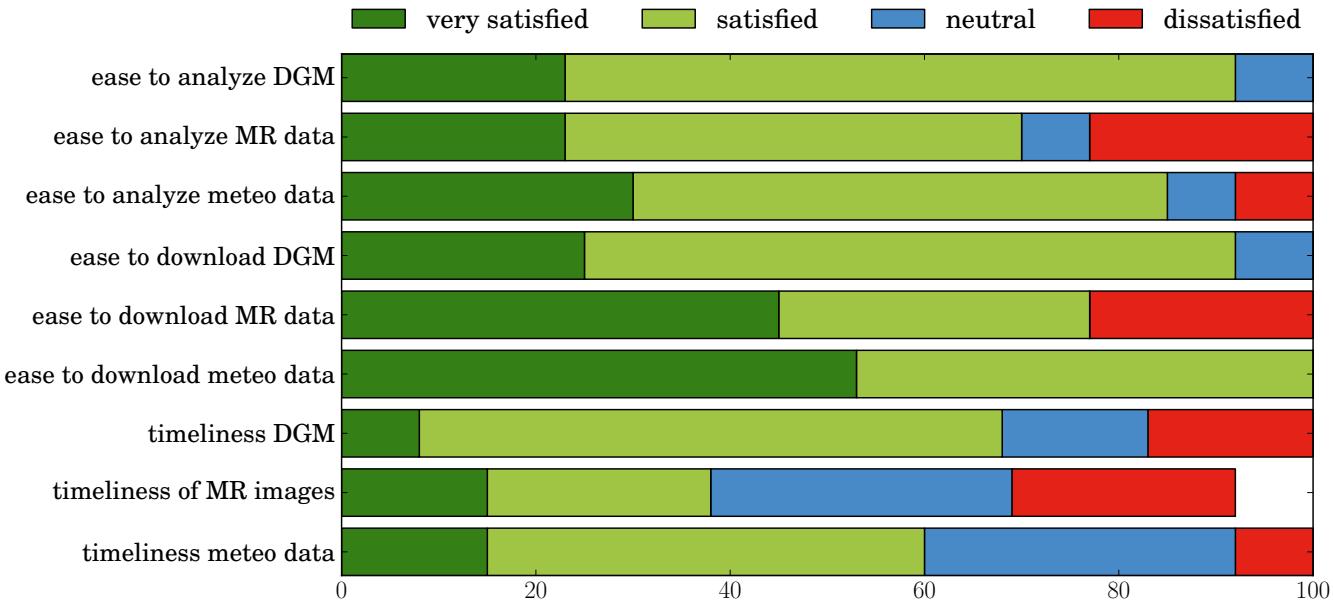

Figure 8. Results of the user survey. National information officers are generally satisfied about the operational provision of remote sensing products for desert locust monitoring in their countries (online questionnaire, April 2012).

5. Discussion

An in-depth accuracy assessment of an operational remote sensing product is critical to inform the users of the product limitations in order to ensure a sensitive use. The variability of inter- and intra-site accuracy measures demonstrates the importance of the low resolution bias that accounts for up to 60% of the errors. Its importance decreases substantially in well-watered areas during the rainy season. Results highlighted that the F_1-measure decreases proportionally to the edge density. The large distances to the Pareto boundary might suggest a low performance of the algorithm. However, in less fragmented areas, this distance diminishes, indicating then a high performance. A visual inspection of the greenness maps revealed that most errors are associated with mixed pixels and that areas required to be surveyed are correctly flagged even if their spatial patterns are not accurately resolved. Besides,

one may identify exogenous errors that would contaminate the results, such as classification errors in the reference maps, as well as discrepancies in the comparison of daily Landsat images and 10-day MODIS composites. Furthermore, Ould Babah [64] concluded that even high resolution images, such as Landsat, were inappropriate to discriminate vegetation in certain Saharan and Sahelian-Saharan environments. The impact of spatial resolution enhancement PROBA-V would ensure both continuation and enhancement of the current monitoring system. A major benefit will be in arid areas associated with winter breeding areas.

The resolution bias appears to be sensitive to the pixel size and the vegetation distribution in the landscape. A link between the accuracy measure and fragmentation has been demonstrated. The spatial structure of vegetation reflects the abiotic characteristics of an ecosystem and influences the functioning, as well as the behavior and the dynamic of animals [65,66]. Additionally, this is particularly relevant for desert locust monitoring. Indeed, meteorological conditions and habitat structure are the two main factors involved in the gathering of solitarious locusts: larvae band migration, mainly driven by wind, is influenced by vegetation density and spatial patterns [67]. Moreover, Despland and Simpson [68] indicated a relationship between landscape fragmentation and locust occurrence: during good breeding years, resources are more abundant and more fragmented. In this line, Ould Babah and Sword [69] found a larger abundance and aggregation of *Panicum turgidum* in a frequently active areas than in a rarely active area. However, the link between vegetation and locust distribution depends on the observation scale [24]. At the scale of an individual plant, vegetation distribution influences gregarization: in a fragmented habitat, desert locusts remain solitarious and swarms do not form [1,70,71]. Conversely, at a large scale, vegetation patterns affect multiplication, concentration and migration [72,73]. Green vegetation favors locust multiplication and allows their numbers to grow. When vegetation enters the senescence phase, it contracts into smaller patches where migrating insects gather to feed [7,74]. Mutual stimulation resulting from the aggregation of solitarious individuals in resource areas leads to gregarization [68,74–76]. Thus, habitat fragmentation concentrates locust populations, increases the chances of contact (and gregarization) and favors recrudescence. In Mauritania, the vegetation distribution varies along the season, and vegetation contraction only appears during years of good locust breeding [24], as this favors gregarization.

To measure the operational impact of those findings, the bio-geographical cycle of the locust and the regions associated need to be considered. The dynamic greenness maps allow reliable vegetation detection in summer breeding areas. According to Ould Babah and Sword [69], the south and southwest represent the main if not the only breeding area. The identification of the potential habitat at that period and the survey of the identified areas will evaluate the number of locusts scattered then. Small patches have a secondary role, except at the end of the rainy season, when populations have increased and gather there. Detections are less accurate in winter and autumn breeding areas: numerous fragmented patches are omitted. These areas are mainly survival biotopes (small wadis, floodplains and depressions), not gregarization biotopes. Nonetheless, these remain fundamental for desert locust reproduction and, thus, for monitoring its dynamics. Even if the assessment focused on Mauritania, it is expected that similar findings would be observed in the distribution areas, especially in countries with similar climates, like Sudan, Yemen, Eritrea and Pakistan, which present a strong seasonal duality. As habitat fragmentation

at the landscape scale appears to promote outbreaks [24], the product appears more fit to monitor large breeding areas than contracted crowding areas.

In two years, the dynamic greenness map product has become a very important component of the locust early warning services provided by the NLCCs and FAO DLIS (national and global levels). Indeed, the maps are used operationally by the NLCCs to prioritize areas in the desert that require monitoring, to plan ground surveys and to guide survey and control teams. The pertinent color table flags the most suitable areas for desert locust. In this way, the large and vast areas of the desert that should be checked for desert locust infestations can be reduced, translating into a significant savings in terms of cost, time and effort. The maps are also used to confirm the response of vegetation to known or estimated rainfall in the desert and to ascertain the suitability of ecological conditions for locust breeding, survival and migration. The product provides useful information for understanding the current locust situation and how it developed. This is especially critical in those areas that cannot be surveyed by ground teams due to remoteness, insecurity or inaccessibility. For ground teams in the field, the dynamic greenness maps are an invaluable resource and tool for delimiting potential areas of green vegetation within the vast confines of the desert. It also helps locust forecasters at FAO to make more precise predictions of the scale and timing of desert locust breeding and migration and to provide earlier warning to the international community. Dynamic greenness maps are incorporated into decadal, fortnightly and monthly locust bulletins produced by NLCCs and distributed to ministries, national agencies, research institutes, NGOs, embassies and donors, the general public and other interested parties. Analysis of the maps is reflected in the monthly FAO Desert Locust Bulletin, as well as warnings, updates and alerts issued by DLIS and made available to nearly 200 Member Countries and donors. Such a rapid and broad uptake by the users can be attributed to the multiple interactions between users and producers along the development phase.

6. Conclusions

This paper aimed at assessing the relevance of the dynamic greenness map product for near real-time operational monitoring of the desert locust habitat. The methodology is based on a colorimetric transformation and a set of thresholds defined by statistical sampling. This study confirmed the robustness of the product in desert locust habitats, but noted that it was less reliable in areas of sparse vegetation, mainly due to the technological limitations of the sensor spatial resolution. The validation acknowledged its suitability for monitoring the seasonal vegetation response during the rainy season corresponding to the summer breeding habitat, which is the most important to monitor. Nevertheless, it does not allow an accurate mapping of the vegetation patches resulting from more sporadic rainfalls. The importance of landscape fragmentation has also been highlighted: the more diffuse the vegetation, the more robust the detection. The resolution strongly affects the detection of contracted vegetation patches. It is anticipated that this shortcoming can be overcome by using the next generation of satellites. Accuracy assessment has highlighted that the PROBA-V sensor will considerably increase the product accuracy. Its improved spatial resolution will reduce by 20% the resolution bias in fragmented areas, allowing better vegetation discrimination. The major benefit will be in arid areas associated with winter

breeding areas. With the introduction of the dynamic greenness maps, the national locust programs in affected countries have become more efficient and cost effective.

Acknowledgments

The authors would like to thank all the reviewers for their relevant comments and suggestions that helped in improving the overall quality of the paper. The authors thank the Centre National de Lutte AntiAcridienne and all its members for their support. We would like to thank Sophie Coremans for reviewing the manuscript before submission.

Author Contributions

All of the authors conceived of and designed the study. Furthermore, François Waldner performed the field campaign under the supervision of Mohamed Abdallahi Babah Ebbe, produced the results.

Conflicts of Interest

The authors declare no conflict of interest.

References

1. Collett, M.; Despland, E.; Simpson, S.J.; Krakauer, D.C. Spatial scales of desert locust gregarization. *Proc. Natl. Acad. Sci. USA* **1998**, *95*, 13052–13055.
2. Steedman, A. *Locust Handbook*; Institute, Overseas development Natural Resources: London, UK, 1988.
3. Brader, L.; Djibo, H.; Faye, F.G.; Ould Babah, M.A.; Ghaout, S.; Lazar, P.M.; Nguala, M. *Towards a More Effective Response to Desert Locusts and Their Impacts on Food Security, Livelihood and Poverty. Independent Multilateral Evaluation of the 2003–2005 Desert Locust Campaign*; Food and Agriculture Organization (FAO): Rome, Italy, 2006.
4. Belayneh, Y.T. Acridid pest management in the developing world: A challenge to the rural population, a dilemma to the international community. *J. Orthoptera Res.* **2005**, *14*, 187–195.
5. Uvarov, B.P. *Grasshoppers and Locust*; Cambridge University Press: Cambridge, UK, 1966.
6. Lecoq, M.; Mestre, J. *La Surveillance des Sautériaux du Sahel*; CIRAD/PRIFAS: Montpellier, France, 1988; Volume 2, p. 32.
7. Roffey, J.; Popov, G. Environmental and behavioural processes in a desert locust outbreak. *Nature* **1968**, *219*, 446–450.
8. Hay, S. Remote-sensing and disease control: Past, present and future. *Trans. R. Soc. Trop. Med. Hyg.* **1997**, *91*, 105–106.
9. Duranton, J.F.; Lecoq, M. *Le Criquet Pèlerin au Sahel;*; Ministère des Affaires Étrangères des Pays-Bas et CIRAD/PRIFAS: Montpellier, France, 1990; Volume 6, p. 84.
10. Popov, G.B. *Etude Écologique des Biotopes du Criquet pèlerin Schistocerca Gregaria (Forskål, 1775) en Afrique Nord Occidentale. Mise en Évidence et Description des Unités Territoriales Écologiquement Homogènes*; CIRAD-PRIFAS: Montpellier, France, 1991; p. 744.

11. Elliott, C.C.H. *FAO's Perspective on Migratory Pests*; Plant Production and Protection Division (AGPP), Food and Agriculture Organization (FAO): Rome, Italy, 1999.
12. Popov, G.B. *Ecological Studies on Oviposition by Swarms of the Desert Locust (Schistocerca Gregaria Forskal) in Eastern Africa*; Anti-Locust Research Center: London, UK, 1958.
13. Uvarov, B.P. The aridity factor in the ecology of desert locust and grasshoppers of the old world. In *Arid Zone Research*; UNESCO: Paris, France, 1957; Volume 8, pp. 164–198.
14. Noy-Meir, A. Desert ecosystems: Environment and producers. *Annu. Rev. Ecol. Syst.* **1973**, *4*, 25–51.
15. Bennet, L. The development and termination of the 1968 plague of the Desert Locust Scistocerca gregaria (Forksal) (Orthoptera, Acrididae). *Bull. Entomol. Res.* **1976**, *66*, 511–552.
16. Cressman, K. *Dynamic Greenness Maps, a Brief Report on Usage for Desert Losut Early Warning*; Food and Agriculture Organization (FAO): Rome, Italy, 2012.
17. Kibasa, R. *Use of SPOT 5 Image to Identify Presence of Locusts*; International Institute for Geoinformation Science and Earth Observation: Enschede, The Netherlands, 2006.
18. Hielkema, J. Satellite environmental monitoring for migrant pest forecasting by FAO: The ARTEMIS system. *Philos. Trans. R. Soc. B Biol. Sci.* **1990**, *328*, 705–717.
19. Pedgley, D.E. *Testing Feasibility of Detecting Locust Breeding Sites by Satellite. Final Report to NASA on ERTS-1, Experiment*; COPR: London, UK, 1973.
20. Hielkema, J. *Application of Landsat Data in Desert Locust Survey and Control*; Food and Agriculture Organization (FAO): Rome, Italy, 1977.
21. Sinha, P.P.; Chandra, S. Visual analysis of land satellite imageries with reference to growthand decay of vegetation in Western Rajasthan. *Plant Prot. Bull.* **1987**, *39*, 29–31.
22. Hielkema, J.U.; Roffey, J.; Tucker, C.J. Assessment of ecological conditions associated with the 1980/81 desert locust plague upsurge in West Africa using environmental satellite data. *Int. J. Remote Sens.* **1986**, *7*, 1609–1622.
23. Tappan, G.G.; Moore, D.G.; Knausenberger, W.I. Monitoring grasshopper an locust habitats in Sahelian Africa using GIS and remote sensing technology. *Int. J. Geogr. Inf. Syst.* **1991**, *5*, 123–135.
24. Despland, E.; Rosenberg, J.; Simpson, S.J. Landscape structure and locust swarming : A satellite's eye view. *Ecography* **2004**, *3*, 381–391.
25. Cherlet, M.; Mathoux, P.; Bartholomé, E.; Defourny, P. SPOT-VEGETATION contribution to Desert Locust habitat monitoring. In Proceedings of the VEGETATION 2000 Conference, Lake Maggiore, Italy, 3–6 April 2000; pp. 247–257.
26. Ceccato, P. Operational early warning system using SPOT-VGT and TERRA-MODIS to predict desert locust outbreaks. In Proceedings of the 2nd VEGETATION International Users Conference,Antwerp, Belgium, 24–26 March, 2005; pp. 24–26.
27. Huete, A.R. Soil influence in remotely sensed vegetation canopy spectra. In *Introduction to the Physics and Techniques of Remote Sensing*; Asrar, G., Ed.; Wiley-Interscience: New York, NY, USA, 1987; pp. 107–141.

28. Gutman, G.G. On the use of long-term global data of land reflectance and vegetation indexes derived from the advanced very high resolution radiometer. *J. Geophys. Res.* **1999**, *104*, 6141–6255.
29. Holben, B. Characteristics of maximum-value composite images from temporal AVHRR data. *Int. J. Remote Sens.* **1986**, *7*, 1417–1434.
30. Pekel, J.F.; Ceccato, P.; Vancutsem, C.; Cressman, K.; Vanbogaert, E.; Defourny, P. Development and Application of Multi-Temporal Colorimetric Transformation to Monitor Vegetation in the Desert Locust Habitat. *IEEE J. Sel. Top. Appl. Earth Obs. Remote Sens.* **2010**, *4*, 318–326.
31. Ceccato, P.; Gobron, N.; Flasse, S.; Pinty, B.; Tarantola, S. Designing a spectral index to estimate vegetation water content from remote sensing data (Part 1: Theoretical approach). *Remote Sens. Environ.* **2002**, *82*, 188–197.
32. Pekel, J.F.; Cressman, K.; Ceccato, P.; Vancutsem, C.; van Bogaert, E.; Defourny, P. Development and application of multi-temporal colorimetric transformation to monitor vegetation in the desert locust habitat. In Proceedings of the MultiTemp 2009—The fifth International Workshop on the Analysis of Multi-Temporal Remote Sensing Images, Mistic, CT, USA, 28–30 July 2009.
33. Vancutsem, C.; Pekel, J.F.; Bogaert, P.; Defourny, P. Mean compositing, an alternative strategy for producing temporal syntheses. Concepts and performance assessment for SPOT VEGETATION time series. *Int. J. Remote Sens.* **2007**, *28*, 5123–5141.
34. Renier, C.; Waldner, F.; Jacques, D.C.; Babah Ebbe, M.A.; Cressman, K.; Defourny, P. A Dynamic Vegetation Senescence Indicator for Near-Real-Time Desert Locust Habitat Monitoring with MODIS. *Remote Sens.* **2015**, *7*, 7545–7570.
35. Ozer, P. Les lithomÉtÉores en rÉgion sahÉlienne: Un Indicateur Climatique de la dÉsertification. Ph.D. Thesis, Université de Liège, Liège, Belgium, 2000.
36. Thys, E.; Pinzon, J.E.; Brown, M.E.; Slayback, D.A. Age and sex composition of small ruminants at Nouakchott markets, Mauritania. *Small Rumin. Res.* **1996**, *20*, 1133–1135.
37. Thiam, A. The causes of spatial pattern of land degradation risk in southern Mauritania using multitemporal AVHRR-NDVI imagery and field data. *Land Degrad. Dev.* **2003**, *14*, 133–142.
38. Niang, A.J.; Ozer, A.; Ozer, P. Fifty years of landscape evolution in Southwestern Mauritania by means of aerial photos. *J. Arid Environ.* **2008**, *72*, 97–107.
39. Ould Ahmedou, C.A.; Yasuda, H.; Wang, K.; Hattori, K. Characteristics of precipitation in northern Mauritania and its links with sea surface temperature. *J. Arid Environ.* **2008**, *72*, 2243–2250.
40. Boschetti, L.; Flasse, S.; Brivio, P. Analysis of the conflict between omission and commission in low spatial resolution dichotomic thematic products: The Pareto Boundary. *Remote Sens. Environ.* **2004**, *91*, 280–292.
41. Bauer, H.L. The statistical analysis of chaparral and other plant communities by means of transect samples. *Ecology* **1943**, *24*, 45–60.
42. McIntyre, G. Estimation of plant density using line transects. *J. Ecol.* **1953**, *41*, 319–330.
43. Buckner, D.L. *Point-Intercept Sampling in Revegetation Studies: Maximizing Objectivity and Repeatability*; American Society for Surface Mining and Reclamation: Denver, CO, USA, 1985.

44. Babah Ebbe, M. Biogéographie du Criquet pèlerin, Schistocerca gregaria Forskål, 1775 : Identification, CaractÉrisation et Originalité d'un Foyer Grégarigène en Centrale, Mauritanie. Ph.D. Thesis, École Pratique des Hautes Études de Paris, EPHE, Paris, France, 2008.
45. Congalton, R.G. A review of assessing the accuracy of classifications of remotely sensed data. *Remote Sens. Environ.* **1991**, *37*, 35–46.
46. Stehman, S.V. Selecting and interpreting measures of thematic classification accuracy. *Remote Sens. Environ.* **1997**, *89*, 77–89.
47. Cohen, J. A Coefficient of Agreement for Nominal Scales. *Educ. Psychol. Meas.* **1960**, *20*, 37–46.
48. Lewis, D.D.; Gale, W.A. A Sequential Algorithm for Training Text Classifiers. *ACM SIGIR Forum* **1994**, *29*, 10.
49. Labatut, V.; Cherifi, H. Accuracy measures for the comparison of classifiers. In Proceedings of The 5th International Conference on Information Technology, Las Vegas, NV, USA, 7–9 April 2008.
50. Congalton, R.G.; Mead, R.A. A quantitative method to test for consistency and correctness in photointerpretation. *Photogramm. Eng. Remote Sens.* **1983**, *49*, 69–74.
51. Rosenfield, G.H.; Fitzpatrick-Lins, K. A coefficient of agreement as a measure of thematic classification accuracy. *Photogramm. Eng. Remote Sens.* **1986**, *52*, 223–227.
52. Witten, I.H.; Frank, E. *Data Mining: Practical Machine Learning Tools and Techniques*, 2nd ed.; Morgan Kaufmann: Burlington, MA, USA, 2005.
53. Zweig, M.H.; Campbell, G. Receiver-Operating Clinical Medicine (ROC) Plots : A Fundamental Evaluation Tool in. *Clin. Chem.* **1993**, *39*, 561–577.
54. Fawcett, T. Introduction to Receiver Operator Curves. *Pattern Recognit. Lett.* **2006**, *27*, 861–874.
55. Youden, W.J. Index for rating diagnostic tests. *Cancer* **1950**, *3*, 32–35.
56. Eva, H.; Lambin, E. Remote sensing of biomass burning in tropical regions: Sampling issues and multisensor approach. *Remote Sens. Environ.* **1998**, *64*, 292–315.
57. Mayaux, P.; Lambin, E. Estimation of tropical forest area from coarse spatial resolution data: A two-step correction function for proportional errors due to spatial aggregation. *Remote Sens. Environ.* **1995**, *53*, 1–15.
58. Mallinis, G.; Koutsias, N. Comparing ten classification methods for burned area mapping in a Mediterranean environment using Landsat TM satellite data. *Int. J. Remote Sens.* **2012**, *33*, 4408–4433.
59. Pepe, M.; Boschetti, L.; Brivio, P.A.; Rampini, A. Comparing the performance of fuzzy and crisp classifiers on remotely sensed images: A case of snow classification. *Int. J. Remote Sens.* **2010**, *31*, 6189–6203.
60. Vintrou, E.; Desbrosse, A.; Bégué, A.; Traoré, S.; Baron, C.; Lo Seen, D. Crop area mapping in West Africa using landscape stratification of MODIS time series and comparison with existing global land products. *Int. J. Appl. Earth Obs. Geoinf.* **2012**, *14*, 83–93.
61. Sword, G.; Lecoq, M.; Simpson, S.J. Phase polyphenism and preventative locust management. *J. Insect Physiol.* **2010**, *56*, 949–957.
62. McGarigal, K.; Tagil, S.; Cushman, S.A. Surface metrics: An alternative to patch metrics for the quantification of landscape structure. *Landsc. Ecol.* **2009**, *24*, 433–450.

63. Monod, T. *Modes "Contracté" et "Diffus" de la végÉtation Saharienne*; Nabu Press: Charleston, WV, USA, 1954; Volume 3.
64. Ould Babah, M.A. *BiogÉographie du Criquet pÈlerin en Mauritanie. Fonctionnement D'une Aire GrégarigÈne et ConsÉquences Sur L'organisation de la Surveillance et de la Lutte Anti-Acridienne*; Food and Agriculture Organization (FAO): Rome, Italy, 2003; p. 122.
65. Tilman, D.; Kareiva, P. *Spatial Ecology: The Role of Space in Population Dynamics And Interspecific Interactions; Monographs in Population Biology*; Princeton University Press: Princeton, NJ, USA, 1997; Volume 30, p. 368.
66. Hooper, D.U.; Vitousek, P.M. Ecosystem processes the effects of plant composition and diversity on ecosystem processes. *Science* **1997**, *277*, 1302–1305.
67. Culmsee, H. The habitat functions of vegetation in relation to the behaviour of the desert locust Schistocerca gregaria (Forskal) (Acrididae: Orthoptera)—A study in Mauritania (West Africa). *Phytocoenologia* **2002**, *32*, 645–664.
68. Despland, E.; Simpson, S.J. Small-scale vegetation patterns in the parental environment influence the phase state of hatchlings of the desert locust. *Physiol. Entomol.* **2000**, *25*, 74–81.
69. Ould Babah, M.A.; Sword, G.A. Linking locust gregarization to local resource distribution patterns. *Environ. Entomol.* **2004**, *33*, 1577–1583.
70. Despland, E.; Collett, M.; Simpson, S.J. Small-scale processes in desert locust swarm formation: How vegetation patterns influence gregarization. *Oikos* **2000**, *88*, 652–662.
71. Despland, E. Fractal index captures the role of vegetation clumping in locust swarming. *Funct. Ecol.* **2003**, *17*, 315–322.
72. Popov, G. *ATlas of Desert Locust Breeding Habitat*; Food and Agriculture Organization of the United Nations: Rome, Italy, 1997.
73. Pedgley, D.E. *Desert Locust Forecasting Manual*; Centre for Overseas Pest Research: London, UK, 1981; Volume 2.
74. Kennedy, J.S. The behaviour of the desert locust (Schistocerca gregaria (Forsk.)) (Orthopt.) in an outbreak center. *Trans. R. Entomol. Soc. Lond.* **1939**, *89*, 385–542.
75. Bouaichi, A.; Simpson, S.J.; Roessingh, P. The influence of environmental microstructure on the behavioural phase state and distribution of the desert locust Schistocerca gregaria. *Physiol. Entomol.* **1996**, *21*, 247–256.
76. Despland, E.; Simpson, S.J. The role of food distribution and nutritional quality in behavioural phase change in the desert locust. *Anim. Behav.* **2000**, *59*, 643–652.